FOCUSED ISSUE FEATURE

Filling the Spectral Holes

Roberto Gómez-García, José P. Magalhães, José-María Muñoz-Ferreras, José M.N. Vieira, Nuno B. Carvalho, and Jeffrey Pawlan

The requirement of wireless access by novel telecommunications and remote-sensing applications, such as Internet-in-mobile services and ultrawideband (UWB) radar systems, is continuously growing in western society but also in countries with big and emerging economies such as China, Brazil, India, and even some African nations [1], [2]. As a consequence, the radio-frequency (RF) spectrum is becoming a very valuable but scarce natural resource. In relation to this, it is well known that some portions of the RF spectrum, such as those assigned to military and emergency services, remain underutilized [3]. These spectral holes, usually referred as "white spaces," then become excellent opportunities for new wireless communications and radar systems to operate. Nevertheless, the necessary dynamic access to properly exploit these free spectral holes can only be performed through very sophisticated and reliable receiver architectures. They must be capable of sensing very broad spectrum ranges while assuring a minimum quality for the received signals. This article addresses modern RF receiver

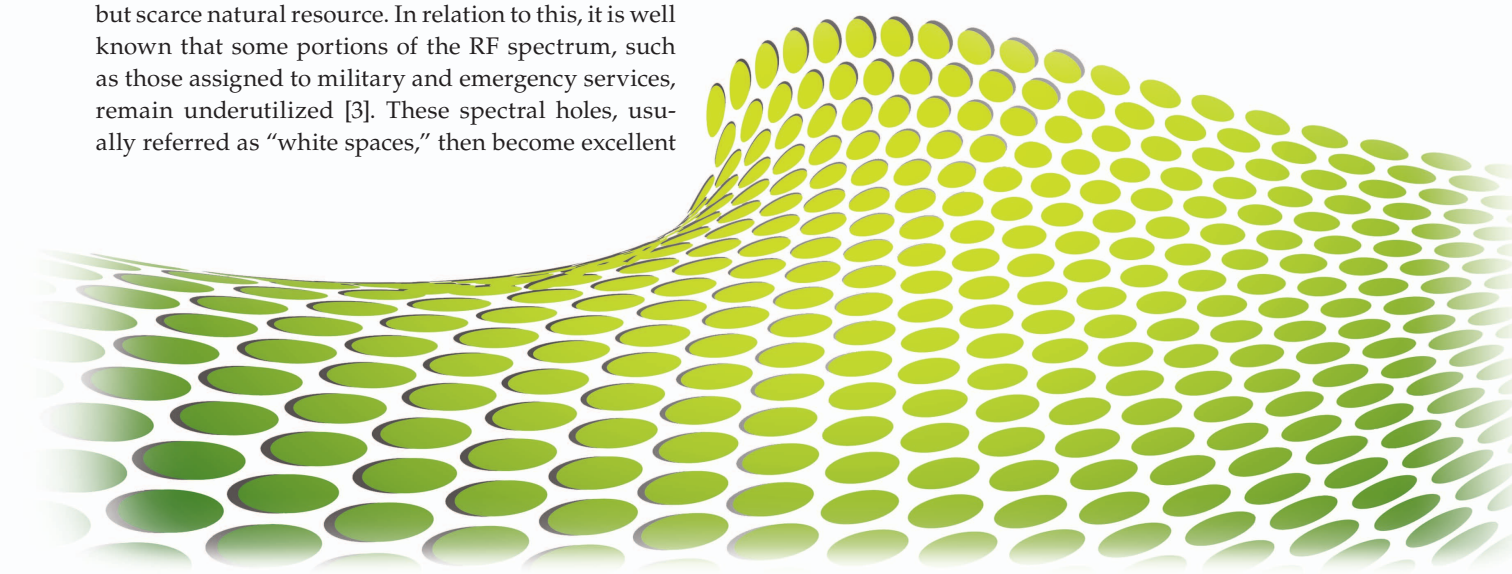

IMAGE LICENSED BY INGRAM PUBLISHING

Roberto Gómez-García (roberto.gomez.garcia@ieee.org) and José-María Muñoz-Ferreras (jm.munoz@uah.es) are with the Department of Signal Theory and Communications, University of Alcalá (UAH), Polytechnic School, Alcalá de Henares 28871, Spain. José P. Magalhães (joseprocha@ua.pt) and Nuno B. Carvalho (nbcarvalho@ua.pt) are with the Departamento de Electrónica, Telecomunicações e Informática (DETI), Instituto de Telecomunicações (IT), Universidade de Aveiro (UA), Aveiro 3810-193, Portugal. José M.N. Vieira (jnvieira@ua.pt) is with the DETI, Instituto de Engenharia Electrónica e Telematica de Aveiro (IEETA), Universidade de Aveiro (UA), Aveiro 3810-193, Portugal. Jeffrey Pawlan (pawlan@ieee.org) is with Pawlan Communications, San Jose, California 95124-4340, United States.

Digital Object Identifier 10.1109/MMM.2013.2296214
Date of publication: 7 March 2014

Channelized mixed-domain receiver architectures have their origin in the concept of hybrid filter bank (HFB) to process the sensed wideband RF signal.

schemes for sensing widebands in communications and radar scenarios.

The problem of wideband sensing for modern receiver configurations, mostly driven by new wireless communications paradigms such as cognitive radio (CR) and software-defined radio (SDR), has been approached mainly from two different perspectives [4]–[6]. These complementary receiver philosophies attend to the way in which the intended broadband portion of the spectrum is captured, as follows:

- Receiver schemes using electronically reconfigurable microwave electronics to acquire such a large bandwidth of the spectrum by continuously sensing smaller portions of it [7], [8]. In these types of receivers, the entire spectral band of interest is explored in subregions instead of in an instantaneous fashion. Examples of key frequency-agile RF components for these receiver schemes encompass tunable bandpass filters for dynamic signal-band selections, adaptive notch filters for interference mitigation, and voltage-controlled oscillators with fixed-frequency bandpass filters to implement an equivalent frequency-controllable signal-capturing process [9]–[12]. Advances here are then limited by the electrical performances achievable by these frequency-adjustable devices; for instance, if reconfigurable bandpass filters are considered, main requisites for their design are the preservation of a high unloaded-quality-factor value within the entire tuning range, which ultimately results in the maintaining of the power insertion loss and selectivity performances throughout it. High switching speed is also mandatory to dynamically sense the whole spectrum in a nearly negligible amount of time, especially in other scenarios such as electronic-warfare applications in battlespace [13]. In the case of adaptive notch filters, the realization of tunable notches for interference suppression while maintaining a broad passband region out of it becomes mandatory for not significantly distorting the signals of interest [14].
- Innovative mixed-mode wideband receiver architectures which hybridize the analog and digital domains [15]. For such receiver alternatives, the full spectral band to be processed is acquired at the same time by fixed-frequency multichannel RF filtering devices—e.g., preselectors consisting of multiplexers or multiband bandpass filters—to be subsequently processed at the digital level [16], [17]. Note that the bottleneck here is the speed-data rate of currently available analog-to-digital converter (ADC) technology, which makes it impossible to directly sample signals occupying UWB spectrum regions [18]–[22]. Indeed, taking into account Moore's law, even if such device exists, it would consume high dc power levels, which would hinder its exploitation in low-power mobile systems [23]. This can be partially circumvented by means of properly conceived receiver solutions, mainly in terms of their filtering stages for signal acquisition so that UWB spectral ranges can be supported by today's commercial ADCs.

On the other hand, a great research effort is being directed toward the development of multiband receiver topologies, not only for wireless communications services but also for radar systems. In SDR applications, as previously outlined, their proper design in terms of multichannel allocation is crucial to considerably alleviate ADC requisites by means of sub-Nyquist direct-sampling principles in mixed-domain receiver configurations. Besides, in remote-sensing scenarios, enhanced capabilities can be attained through multifrequency radar implementations that process target echoes coming from different spectral bands [24]. Among others, target detection [25], [26], automatic target recognition (ATR) algorithms [27]–[29], radar-image fusion [30], automotive configurations [31], subsurface sensing [32], or efficient clutter cancelation in life-detection scenarios [33] are to highlight. In addition, higher robustness to mono-band jamming and unintentional interference phenomenon from other colocated wireless systems may be achieved.

The aim of this overview article is to report the latest research findings in the development of modern receiver architectures for broadband spectrum sensing in wireless communications and radar scenarios. Emphasis is made on mixed-domain broadband and multichannel receiver solutions for telecommunications services in the CR/SDR context. For some of these receiver configurations, their operation features for some types of modulation [e.g., quadrature amplitude modulation (QAM)] are shown. Furthermore, recent trends in the realization of multiband receiver schemes for remote-sensing applications exemplified in linear-frequency-modulated continuous-wave (LFMCW) radars are presented. Specifically, different minimum-hardware multifrequency radar structures are described, and functionality performances in terms of target detection capability for an imaging application are expounded.

Channelized Wideband Mixed-Domain Receivers

Channelized mixed-domain receiver architectures have their origin in the concept of a hybrid filter bank (HFB) to process the sensed wideband RF signal [23], [34], [35].

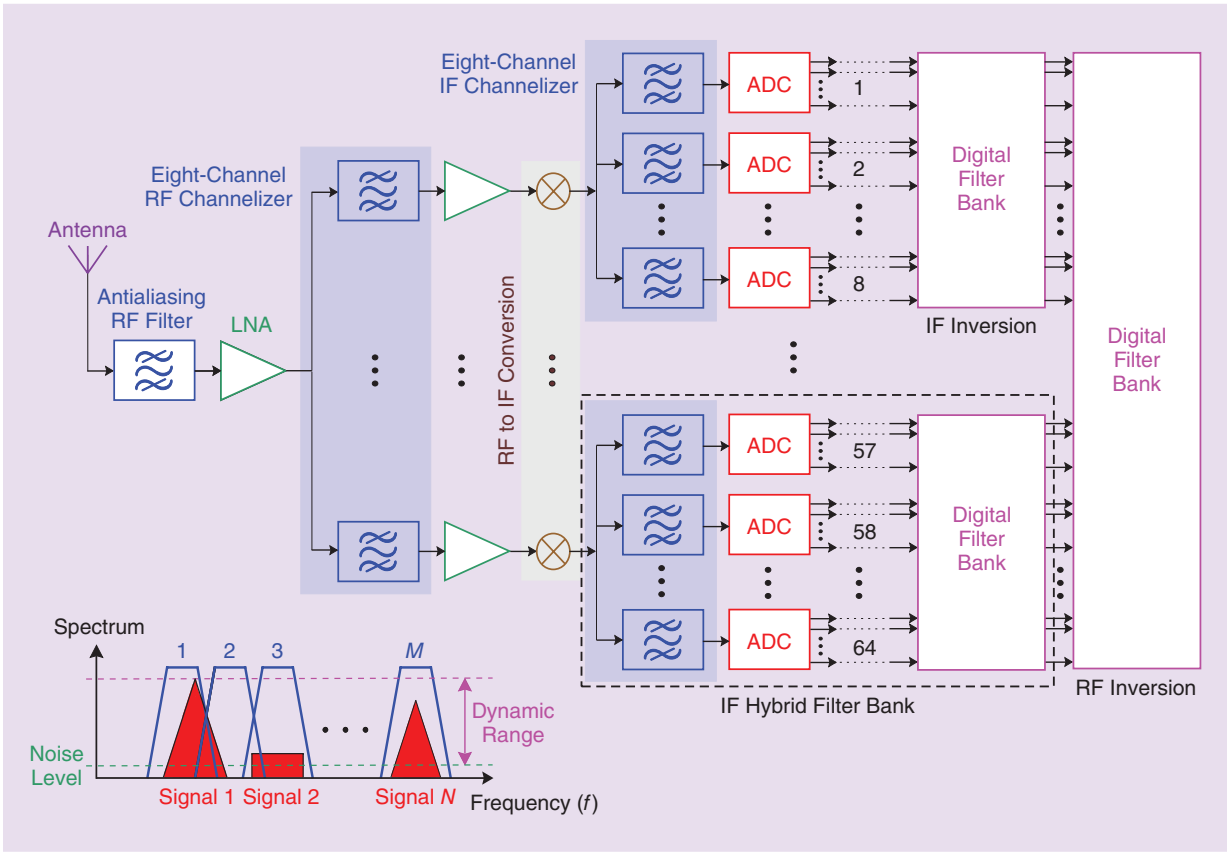

Figure 1. *An example of a channelized wideband mixed-domain receiver with 64 channels [15].*

Figure 1 shows the conceptual block diagram of this kind of receiver for an example of 64 channels [15]. The key feature of this receiver approach, so that it can correctly process the broad frequency range sensed by the antenna, is the exhaustive signal-spectrum channelization into multiple frequency-narrower subbands. This is done here by two stages at the RF and IF levels. First, the signal spectrum captured by the antenna is split after antialiasing filtering and amplification into several bands—eight in this case—by an RF channelizer. After that, once these signals components have been down-converted in parallel to the same IF range, they are further subdivided into various subbands—eight again in this example—by the intermediate frequency (IF) preselector. Thus, they can be sampled by less-demanding ADCs for their subsequent processing in the digital domain. It leads to a sampling-rate reduction by a factor equal to the total number of channels regarding a single-ADC receiver directly sampling the whole bandwidth. Thus, the basic task of the two-stage channelizing procedure of this receiver is to accommodate such a large portion of the electromagnetic spectrum to commercially available ADC technology.

Several remarkable advantages are found in this mixed-domain wideband receiver approach when compared to more traditional fully analog receiver architectures for wireless communications systems:

- The dynamic-range figure of merit is noticeably improved due to the wideband channelization process since low-power signals can be detected in the presence of high-power signals as long as they appear allocated at different spectral regions (see the lower left part of Figure 1). Consequently, blocking-effect robustness is also enhanced.
- Hardware imperfections having their origins in different phenomenons, such as the finite selectivity of the analog filters embodied in the channelizers that gives rise to aliasing and distortion terms during sampling, can be corrected at the digital level by the synthesis digital filter banks. Note also that, in this receiver scheme, the digital part can be readapted or reconfigured in real time. This feature permits to dynamically compensate other undesired effects that could arise making imprecise the analog circuits in relation to their ideal models, such as manufacturing tolerances, temperature drifts, or parasitic coupling.
- The overall system dc-power consumption is decreased with regard to a single-ADC receiver implementation handling the same bandwidth. This is because those branches of the channelized receiver that are not utilized at a specific time for spectrum reconstruction can be temporarily turned off.

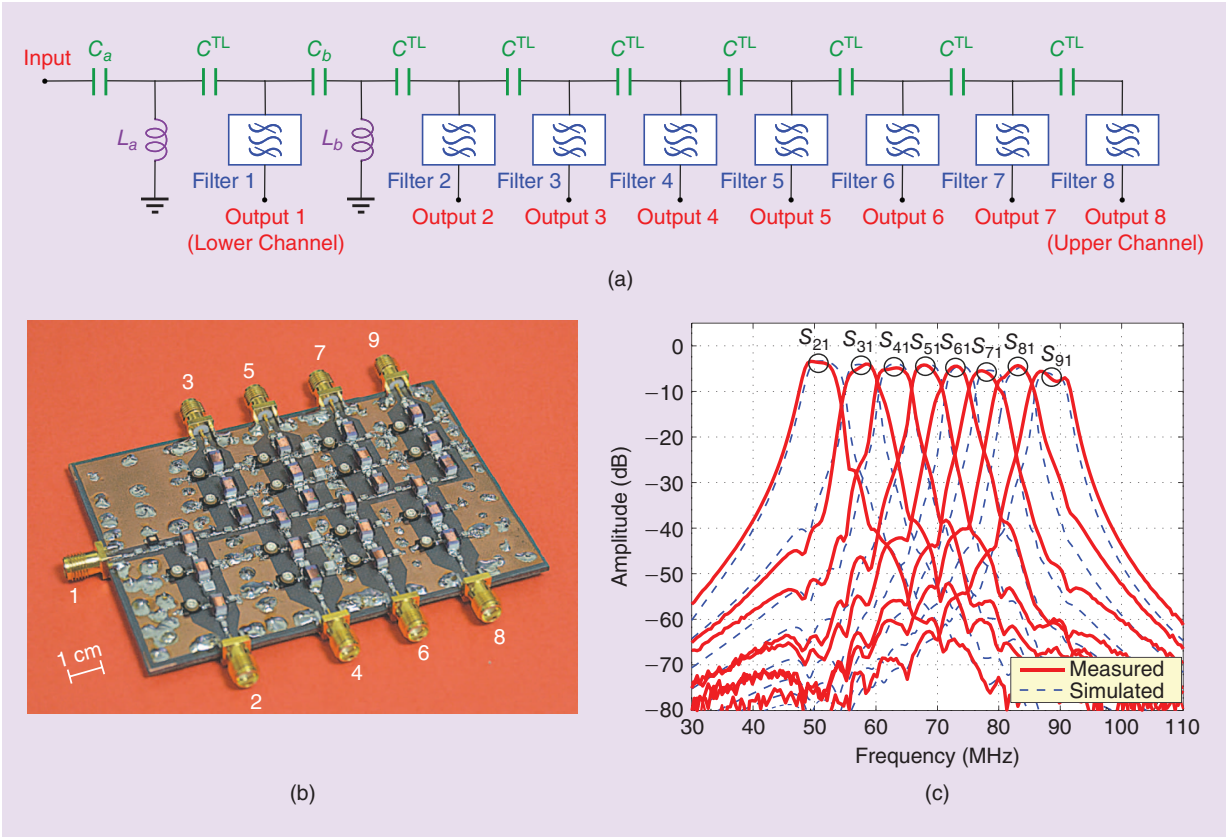

Figure 2. *An example of an eight-channel IF lumped-element channelizer based on an inverted-cochlea approach [16]. (a) The circuit scheme, (b) a photograph, and (c) simulated and measured power transmission responses for the channel.*

- Parallelized multiband signal processing and environment adaptivity are intrinsic characteristics to this kind of receiver.

The most critical elements in the devised mixed-domain receiver arrangement are the RF and IF channelizers or preselectors carrying out the captured signal-spectrum division into multiple subbands. Furthermore when broader regions of the spectrum are intended to be sensed, which irremediably leads to more challenging multiplexer designs involving a higher number of wider-bandwidth channel filters. Obviously, owing to practical aspects, different solutions must be adopted for the RF and IF channelizers, as follows:

- Planar technologies, such as microstrip, stripline, or coplanar waveguide, are a preferred choice for the RF multiplexer design. Since this class of receivers is projected to be mainly exploited in the lower part of the microwave band, a waveguide-based or coaxial-cavity realization is not appropriate due to size/weight constraints and the absence of high power-handling capability needs [36], [37]. Besides, the channel filters should be spectrally adjacent each to the other, so that no frequency regions of the captured signal are lost. Such a stringent contiguous-channel requisite could hardly be afforded in preselector devices with a large number of branches, owing to difficulties inherent to the interchannel isolation process for wideband designs. Indeed, only a few alternatives suitable for such high-frequency multiplexers, based on manifold arrangements and multistar/ring junctions, have been proposed [16], [38], [39]. The development of these RF filter banks in miniaturized technologies to achieve higher circuit-size compactness, such as microelectromechanical systems (MEMs) or surface-acoustic-wave (SAW) and bulk-acoustic-wave (BAW) resonators, is currently acquiring a great interest.
- For the IF channelizer, a lumped-element implementation is the best option in terms of electrical performance. Nevertheless, integrated multiplexing devices made up of g_m-C filters could be also be advantageous regarding occupied area. Design constraints here are related with the availability of only some nominal values for commercial discrete elements and their tolerances. An interesting structure to realize this multiplexer is the so-called cochlea-based configuration [40], [41]. It is a bioinspired circuit that mimics the sound-acquisition mechanism of the mammalian cochlea of the human hearing system. As an example of a proof-of-concept manufactured prototype, Figure 2 shows an inverted version of

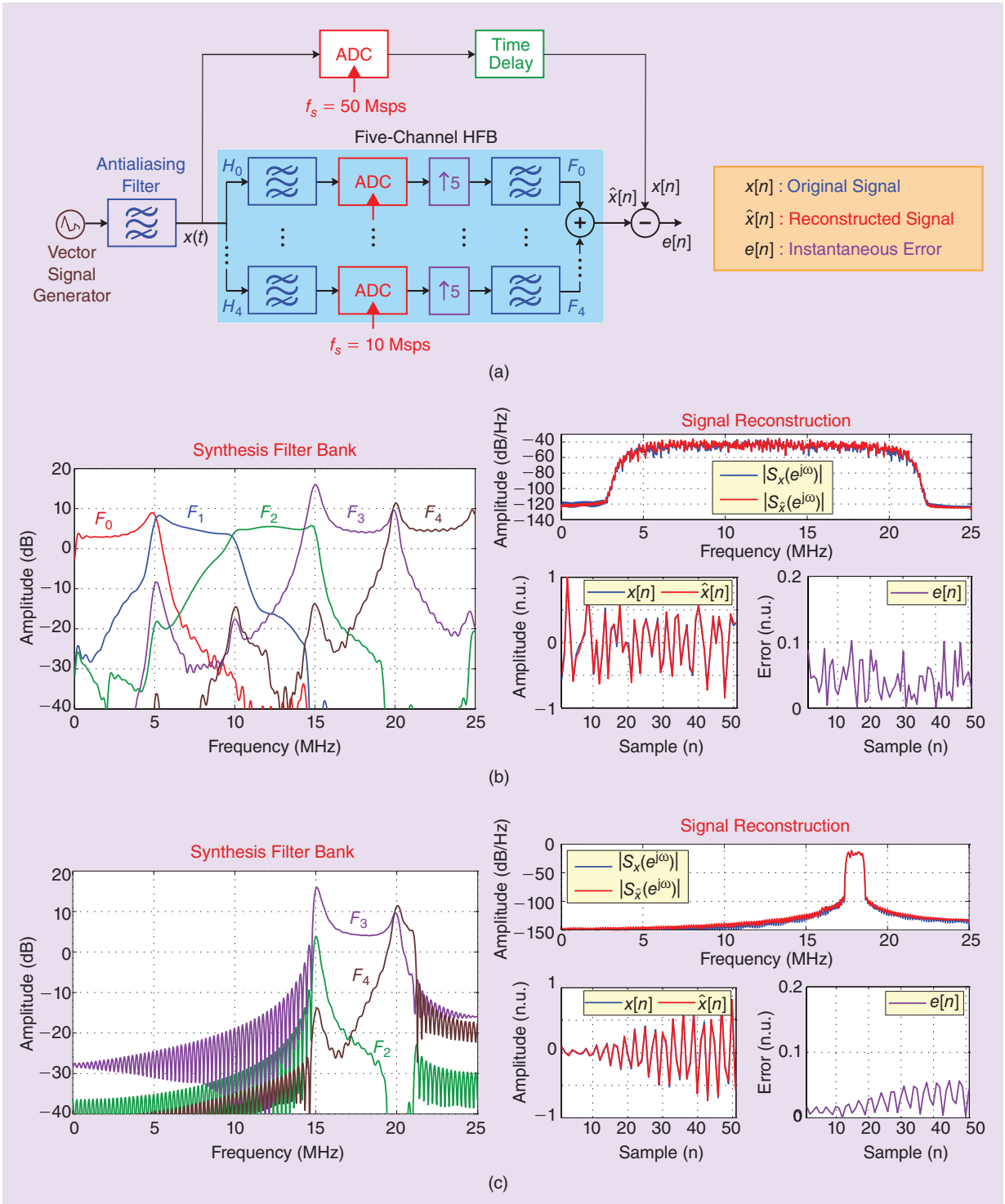

Figure 3. *The signal-reconstruction examples. (a) Experimental setup. (b) 16-QAM wideband signal. (c) 16-QAM narrowband signal [47].*

such a multiplexer for an eight-channel design covering the 50–100-MHz band circuit detail, photograph, and simulated and measured power transmission responses for its channels [16].

On the other hand, digital filter banks are also basic blocks in the suggested mixed-mode wideband receiver. As explained, they perform a double functionality in the HFB: 1) aggregation of the signal subbands to reconstruct the overall signal in the digital domain and 2) compensation of the distortion and aliasing terms caused by the sampling process and influenced by hardware nonidealities. Performances in their operation are related with the specific signal-reconstruction algorithm programmed in them;

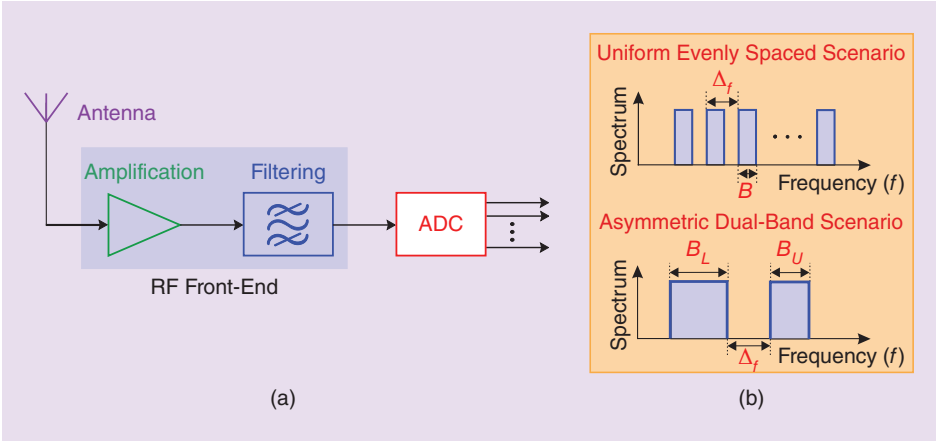

Figure 4. *A sub-Nyquist direct-sampling multichannel receiver. (a) The architecture scheme and (b) multi- and dual-band scenarios.*

examples include maximally decimated or oversampled HFB techniques, as well as limitations related to the computational cost of the field-programmable gate array (FPGA) implementation of the digital filter impulse responses [42]–[46].

To conclude, the correct operation of the mixed-domain receiver is evaluated through two signal-reconstruction experiments [47]. These tests have been conducted in the IF HFB by only considering the five lower channels of its IF channelizer of Figure 2, which span from 50 MHz up to 75 MHz, i.e., 25 MHz of overall signal bandwidth to be handled. The setup of the experimental procedure for the signal-reconstruction tests, along with the obtained results for a wideband and a narrow-band signal, are shown in Figure 3. The evaluation consisted in the comparison of the IF part of the channelized mixed-domain receiver architecture and its equivalent single-ADC receiver directly sampling the same signal bandwidth. Specifically, two signals are compared in each test: the reconstructed signal and the original one as acquired by the classic receiver. In these experiments, the sampling rate in each ADC is 10 megasamples per second (Msps), i.e., five times lower than the minimum one imposed by the Nyquist theorem and used by the direct-sampling receiver. To generate the real-time signals, an SMU200A vector signal generator from Rohde & Schwarz was utilized. A maximally decimated structure for the IF HFB with inversion digital filters optimized through the Papoulis–Gerhberg algorithm was synthesized. There were 200-coefficient impulse responses that were assumed for the digital filters. More details about these experiments and the obtained results are as follows:

- The wideband example uses a 16-QAM signal with a rate of 20 megasymbols per second (Msymb/s) and a carrier frequency of 62.5 MHz. The reconstructed and original signals attained after using the five digital filters in the channelized approach (F_0, F_1, F_2, F_3, and F_4), which are compared in both frequency and time domain, show a fairly close agreement. In the time domain, the computed deviation mean error in normalized-to-the-maximum absolute terms is 0.05.
- The narrow-band example consists of a 16-QAM signal with a symbol rate of 1 Msymb/s and a carrier frequency of 68 MHz. In this case, only those digital filters of the channelized solution near or inside the band of interest (F_2, F_3, and F_4) are employed in the reconstruction process. The attained reconstruction results in frequency and time domain for the narrow-band signal lead to a reconstruction error even lower than in the previous wideband example, of about 0.025 in normalized terms.

Sub-Nyquist Direct-Sampling Multichannel Receivers

Conventional CR/SDR receiver approaches reported in the technical literature exhibit different limitations, as follows:

- Superheterodyne architectures, which commonly suffer from great size, need for careful designs to avoid problems related to image bands and spurious signals resulting from the use of mixers in signal down-conversion stages [48]. This drawback can be extrapolated to the channelized wideband mixed-domain receiver structure expounded in the previous section (see Figure 1).
- In zero-IF receiver configurations, in-phase/quadrature imbalances and dc offsets could be very critical [49]–[51].
- Low-IF receiver arrangements have the same drawbacks of the latter and the image-frequency disadvantage of superheterodyne receivers [49]–[51].

One interesting alternative to overcome the aforementioned shortcomings is the direct-sampling architecture, which employs an ADC just after filtering the input RF spectrum captured by the antenna [52]–[55]. However,

as it was pointed out, commercially available ADC technology does not allow to process excessively large RF acquisition bandwidths due to restrictions on feasible maximum speed-data rates. This is the bottleneck of this receiver concept when applied to broadband sensing.

Fortunately, the multiband functionality and channel simultaneity may be met in this direct-sampling receiver principle by incorporating on it a high-frequency multipassband filter and a simpler ADC sampling at a sub-Nyquist rate. This is depicted in Figure 4. The idea behind this approach is that a sparse spectrum does not need to be sampled at the Nyquist rate to be properly acquired (i.e., without aliasing). Indeed, like in the mono-band case and according to the bandpass sampling theorem, sampling frequencies below that imposed by the Nyquist criterion may be used here [56]. By doing so, less stringent demands are obtained when operating at the minimum sub-Nyquist sampling rate since only some spectral channels are intended to be acquired. If this minimum sub-Nyquist frequency is to be adopted, some restrictions on the channels positions need to be imposed. The mathematical rules for their proper allocation can be derived not only for evenly spaced equal-bandwidth channels, but also for more general scenarios consisting of multiple bands with arbitrary center frequencies and bandwidths. The complete analytical deduction of these design guidelines can be found in [57] and [58].

It should be remarked that, if the design rules detailed in [57] and [58] for the multichannel spectral allocation are not followed, then irremediable aliasing problems can arise during the sampling process. This is illustrated in Figure 5 for a specific quad-band acquisition scenario [57]. In particular, Figure 5(a) shows the spectrum of a normalized-to-f0 subsampled quad-band signal at a rate equal to the minimum sub-Nyquist sampling frequency $f_{s,\min}$. As can be seen, no overlapping between channels arises in this case—the channel disorder and the possible spectrum inversion are not critical issues, since they can be corrected by the digital postprocessing part. In contrast, aliasing can appear for sampling frequencies higher than

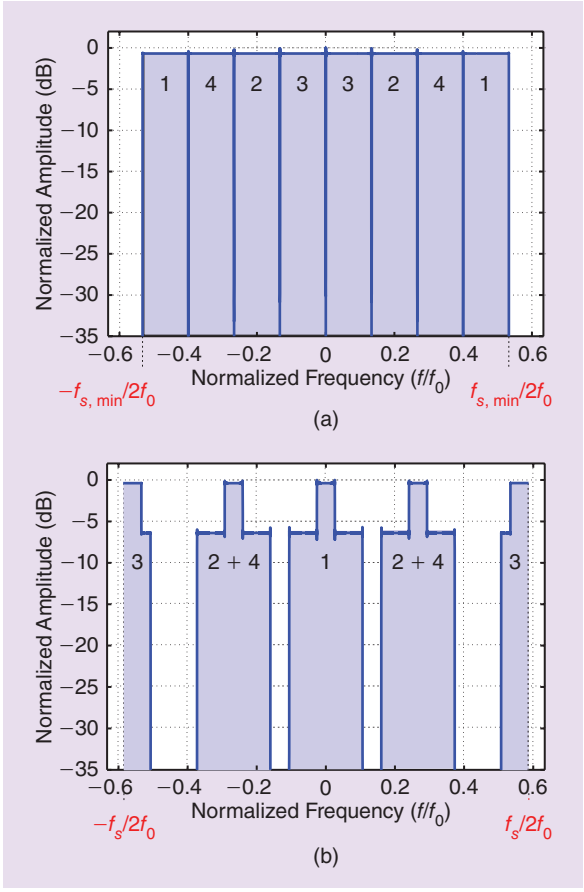

Figure 5. *Examples of (a) no aliasing and (b) aliasing for a quad-band sub-Nyquist direct-sampling receiver [57].*

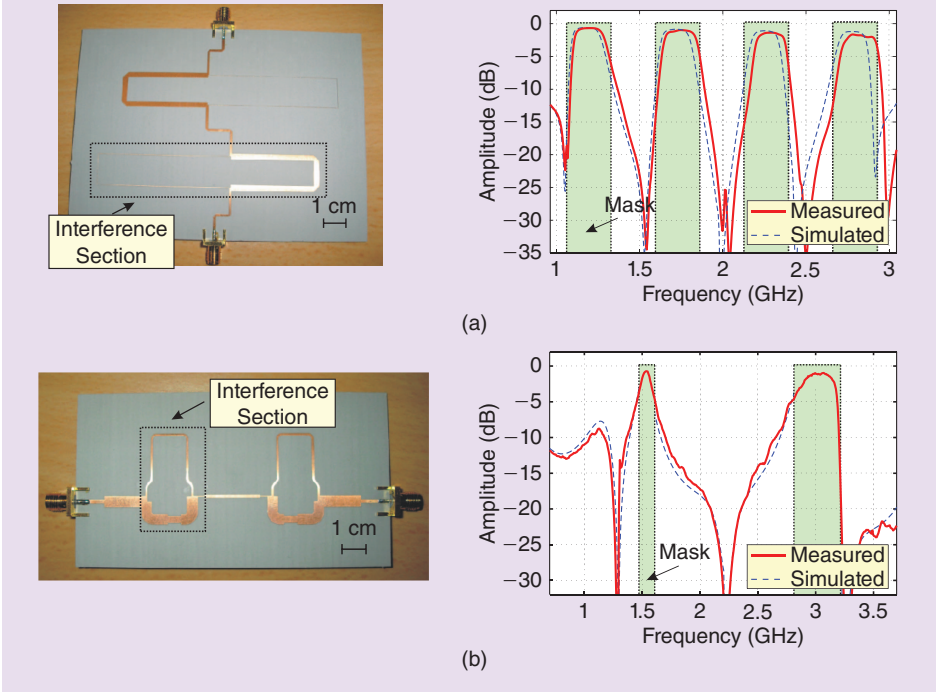

Figure 6. *Examples of signal-interference multipassband microstrip filters for sub-Nyquist direct-sampling multichannel receivers. (a) A quad-passband filter with evenly spaced equal-bandwidth channels [57]. (b) A frequency-asymmetrical dual-passband filter [58].*

This scheme, shown in Figure 8 and also known as "dechirping," simply consists of mixing a replica of the transmitted signal with the received one.

the minimum sub-Nyquist sampling frequency. This is demonstrated in Figure 5(b) for a sampling frequency equal to 1.1 times the latter, where the resulting channel spectral superposition is also indicated.

From a hardware perspective, the core of the sub-Nyquist direct-sampling multichannel receiver of Figure 4 is the multipassband filter. More still after considering that such filtering device could hardly be realized through traditional coupled-resonator circuits, especially if a high number of channels covering a UWB spectral range is required. Indeed, practical implementations of coupled-resonator multiband bandpass filters have been limited to filtering actions with no more than four passbands [59]–[61].

This problem can be circumvented through multiband bandpass filters based on signal-interference techniques [62], [63]. In these circuits, which exploit feedforward signal-interaction principles in transversal multipath topologies to shape the transfer function, high-selectivity filtering profiles with any number of passbands can be produced throughout UWB spectral ranges. As an example, Figure 6 shows two microstrip prototypes of signal-interference multipassband planar filters for sub-Nyquist direct-sampling multichannel receivers—photographs, simulated and measured power transmission responses, and ideal channel masks [57], [58]. The analytical foundations and the design methodology of this type of filters are described in [62] and [63]. More information regarding these circuits and their receiver application is provided below.

- The prototype of Figure 6(a) corresponds to a quad-passband filter for a direct-sampling evenly spaced equal-bandwidth four-channel receiver [57]. The center frequencies for its channels, listed from the lower to the upper one, were selected to be 1.2, 1.73, 2.27, and 2.8 GHz. Their bandwidths were fixed equal to 267 MHz. It can be checked that a sub-Nyquist sampling frequency of 2.134 GHz, which is a much lower value than the 5.867 GHz imposed by the Nyquist theorem, can be used in this case to directly sample these bands without aliasing.
- The prototype of Figure 6(b) consists of a dual-passband filter for a direct-sampling two-channel receiver with strong spectral asymmetry between bands [58]. The lower and upper channels were chosen to be centered at 1.53 and 3 GHz, respectively, with bandwidths of 133 and 400 MHz. In such a case, a minimum sub-Nyquist sampling frequency of 1.067 GHz can be utilized to directly sample these bands without aliasing. Note that, as in the quad-passband filter example, it is a much lower value than the 6.4 GHz resulting from the Nyquist criterion.

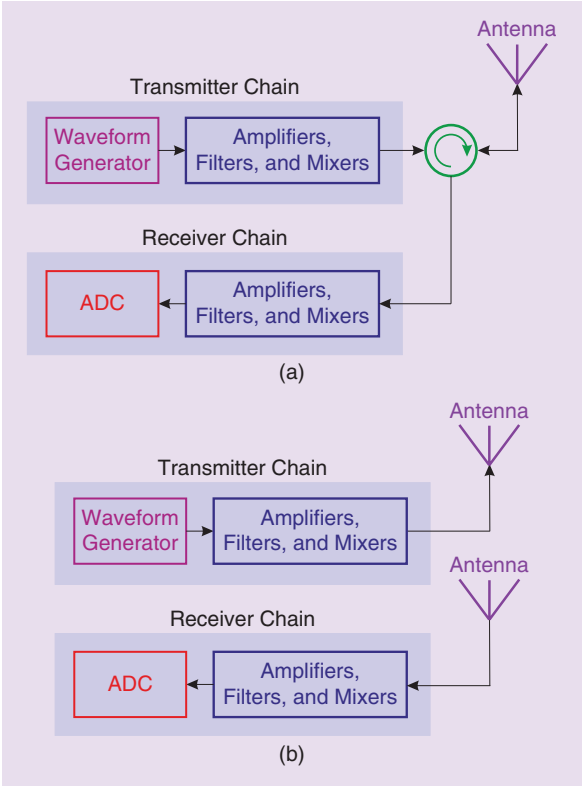

Figure 7. *Standard architectures for a radar system. (a) Circulator scheme for pulsed radars. (b) Two-antenna scheme for CW radars.*

Multiband Radar Receivers

It is well known that radars have a plurality of important applications, such as detection, localization, tracking, and even imaging [24], [64]. Recently, multifrequency radars have arisen. By processing the target echoes coming from different bands, multiband radars can extend and enhance their functionalities, thus outperforming standard mono-band radar sensors [25]–[33]. This is a major justification for the research into innovative receiver architectures for

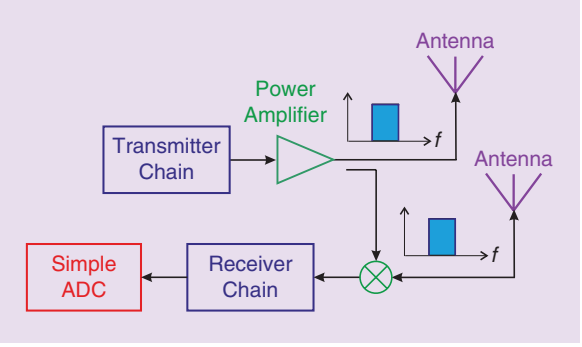

Figure 8. *A scheme for a mono-band LFMCW based on deramping.*

emerging multifrequency radars, especially for continuous-wave (CW) systems. Nevertheless, note that the design of these multiband radars are also motivated by specific requirements, such as those related to target classification, detection, counter-measurement issues, and so forth.

A CW radar transmits a signal all the time, unlike traditional pulsed radars [24], [64]. This implies that the sensitive receiver of a CW radar must simultaneously operate with the transmitter. To improve the isolation between the transmitter and receiver modules, the conventional pulsed-radar configuration with an isolator, such as the one shown in Figure 7(a), is usually avoided for CW radars. In contrast to it, CW radars commonly employ two high-directivity antennas to increase the transmitter-receiver isolation as illustrated in Figure 7(b).

Among CW radars, those using an LFMCW waveform are of great relevance. In addition to obtain a high-range resolution, this waveform has advantageous characteristics in terms of low probability of interception [65]. Furthermore, architectures for LFMCW radars can include an analog deramping stage, which deeply relaxes the speed-data rate requisite for its receiver ADC [66]. This scheme, shown in Figure 8 and also known as "dechirping," simply consists of mixing a replica of the transmitted signal with the received one. At the RF mixer output, the so-called beat signal is obtained. This low-frequency signal has a bandwidth much lower than the transmitted one, thus being much easier to be acquired. Interestingly, this ADC relaxation transforms this type of radars into quasi commercial-off-the-shelf (COTS) prototypes. Some examples to be highlighted are the Brigham Young University microsynthetic aperture radar (μSAR) systems [67], the millimeter-wave high-range-resolution Technical University of Madrid demonstrator [68], or the miniaturized synthetic aperture radar (MISAR) developed to fly on small unmanned aerial vehicles [69].

By combining the deramping concept and the multiband paradigm, two high-level deramping-based solutions for multiband LFMCW radars can be envisaged.

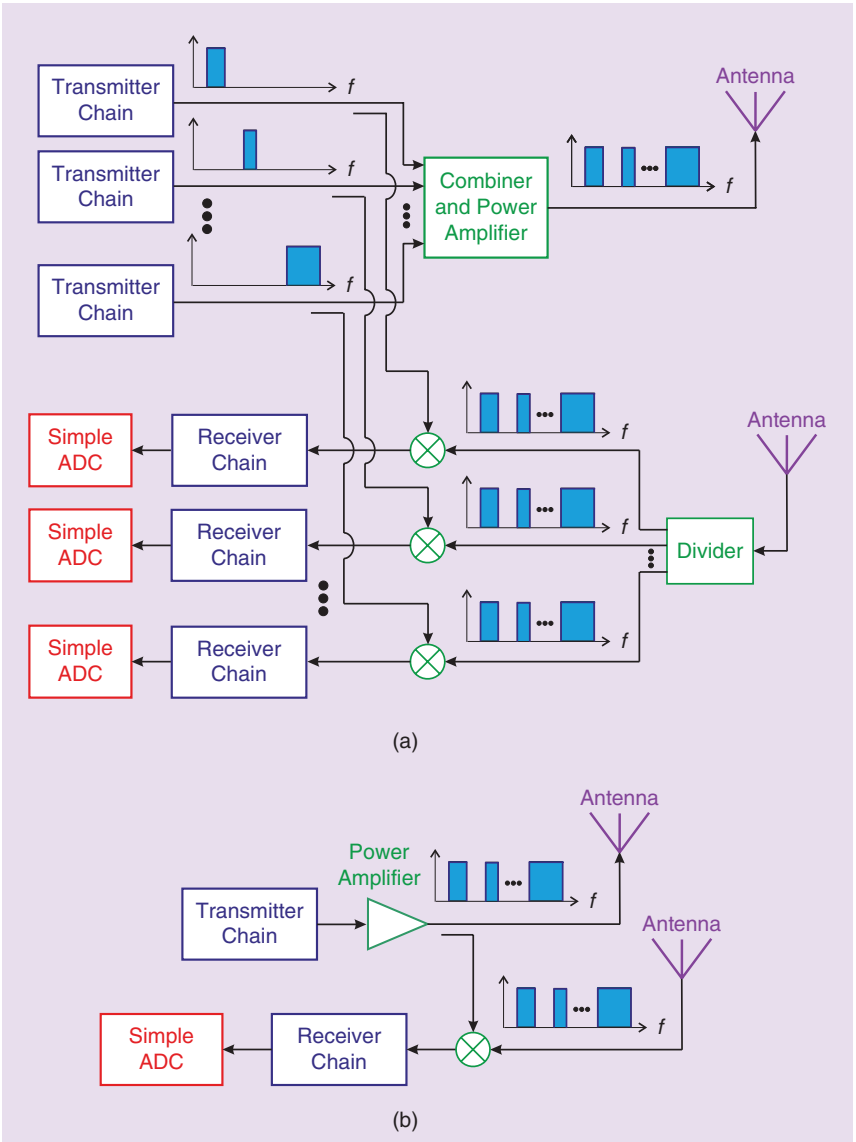

Figure 9. *Deramping-based architectures for a multiband LFMCW radar sensor [75], [76]. (a) A multiple-receiver scheme. (b) A single-receiver scheme.*

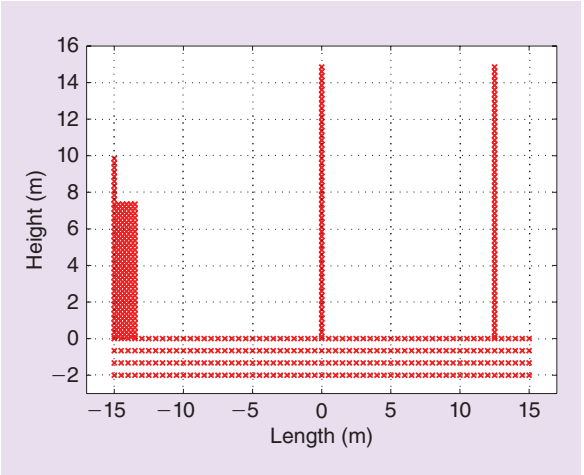

Figure 10. *The scatterer distribution of the maritime target [76].*

Several remarkable advantages are found in this mixed-domain wideband receiver approach when compared to more traditional fully analog receiver architectures for wireless communications systems.

They are shown in Figure 9. Regarding the scheme of Figure 9(a), it is noticeable that a replica of the waveform transmitted in each band is employed for deramping purposes in each receiver path. It becomes easy to understand that the access to this replica can be assured by filtering the transmitted signal or by extracting some energy from each band. In relation to Figure 9(b), it should be emphasized that the radar structure is very compact since it only uses one single low-end ADC. The scheme of Figure 9(b) is a minimum-hardware solution, but has some limitations. Nevertheless, as proven below, they can be circumvented through a proper multiband radar design.

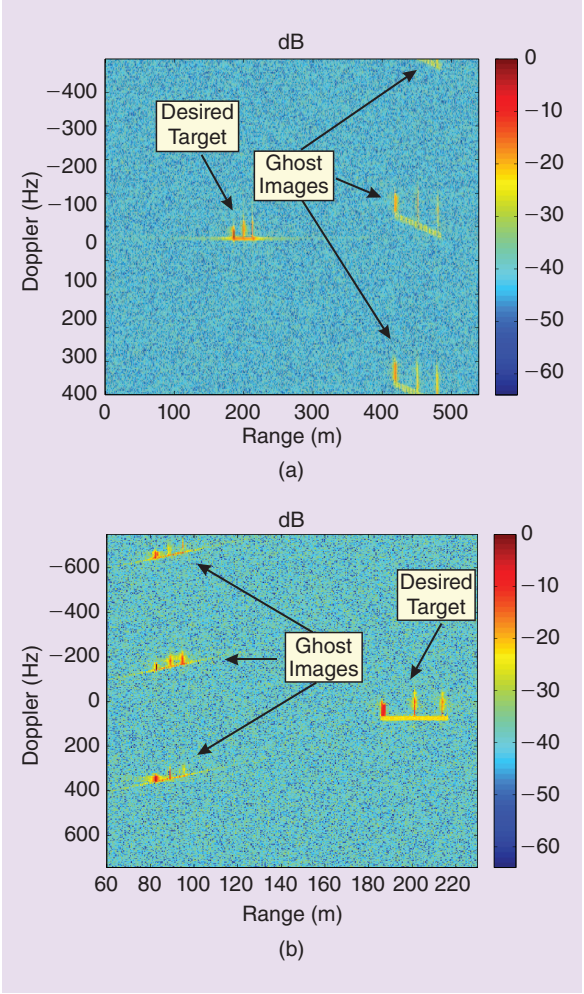

Figure 11. *Simulated ISAR images for the with desired and ghost images [76]. (a) Lower channel. (b) Upper channel.*

An imaging application is now considered to evaluate the proposed multiband radar receivers. Inverse synthetic aperture radar (ISAR) is an interesting technique for which the deramping-based multiband LFMCW radar architectures of Figure 9 can be exploited. ISAR is a coherent radar procedure which enables the generation of images of noncooperative targets, i.e., targets whose motion is unknown [70]. A high-range resolution can be achieved by transmitting a large bandwidth, whereas a fine cross-range resolution depends on a large variation of target aspect angle during the dwell time. ISAR images are range-Doppler projections of the target and the obtained view depends on the relative motion between target and radar [71], [72]. This unknown motion gives rise to undesired defocusing effects, which can be mitigated by means of translational and rotational motion compensation approaches also valid to the multiband case [73], [74].

For the preferred minimum-hardware deramping-based radar architecture of Figure 9(b), although only one single beat signal is available, an ISAR image can be formed for each band. The procedure is exhaustively detailed in [75] and [76]. To show how it works, let it consider the simulation of a maritime target, whose spatial distribution of scatterers is given in Figure 10. The target is assumed to be illuminated by a dual-band LFMCW radar, whereas it is pitching and moving along the radar line-of-sight. Note that this motion eventually produces a side-view ISAR image.

Figure 11 represents the obtained ISAR images for the lower and upper bands. Note that, in addition to the desired image, several ghost images appear. Fortunately, through the proper selection of the radar parameters, these images appear at other ranges and do not mean any interference for the wanted target. Thus, they are not problematic. Note also that no ghost images appear with the more complex architecture of Figure 9(a).

Summary and Conclusion

This overview article has presented recent contributions in the field of advanced wideband receiver configurations for telecommunications and remote-sensing applications. Two different approaches of mixed-domain receivers for wireless communications systems in the CR/SDR scenario have been described. The first receiver structure exploits the exhaustive channelization of the full sensed spectrum under the HFB philosophy. This is carried at two levels through RF and IF multiplexers, so that the captured signal can be accommodated to be processed by low-cost ADCs through its division into multiple subbands. Performance evaluation has been carried out by means of two reconstruction experiments for QAM signals. The second receiver architecture operates in a properly designed frequency-sparse region of the spectrum in terms of center frequencies and bandwidths for their channels. Thus, the sensed

signal bands can be directly sampled at sub-Nyquist rates after being selected with signal-interference multiband bandpass filters as key components of this sort of receiver. For radar sensors, innovative multiband receiver arrangements for LFMCW systems have been suggested. Special attention has been paid to minimum-hardware multifrequency radar schemes. Furthermore, their operative performances have been compared in terms of target detection capability for a maritime imaging application.

Acknowledgment

This work has been supported by the University of Alcalá under the research project CCG2013/EXP-038.

References

[1] D. Raychaudhuri and N. B. Mandayam, "Frontiers of wireless and mobile communications," *Proc. IEEE*, vol. 100, no. 4, pp. 824–840, Apr. 2012.

[2] J. D. Bryan, J. Kwon, N. Lee, and Y. Kim, "Application of ultra-wide band radar for classification of human activities," *IET Radar, Sonar Navig.*, vol. 6, no. 4, pp. 172–179, Mar. 2012.

[3] P. S. Ryan, "Some tests of spectrum usage in Brussels," Univ. Colorado at Boulder, Boulder, CO, Tech. Rep., 2004. [Online]. Available: http://www.legislation.eu/upload/dossier/doc/126-1.pdf

[4] J. Mitola, "The software radio architecture," *IEEE Commun. Mag.*, vol. 33, no. 5, pp. 26–38, May 1995.

[5] R. Bagheri, A. Mirzaei, M. E. Heidari, S. Chehrazi, M. Lee, M. Mikhemar, W. K. Tang, and A. A. Abidi, "Software-defined radio receiver: Dream to reality," *IEEE Commun. Mag.*, vol. 44, no. 8, pp. 111–118, Aug. 2006.

[6] P. Cruz, N. B. Carvalho, and K. A. Remley, "Designing and testing software-defined radios," *IEEE Microwave Mag.*, vol. 11, no. 4, pp. 83–94, June 2010.

[7] L. Larson, S. Abdelhalem, C. Thomas, and P. Gudem, "High-performance silicon based RF front-end design techniques for adaptive and cognitive radios," in *Proc. 2012 IEEE Compound Semiconductor Integrated Circuit Symp.*, La Jolla, CA, Oct. 14–17, 2012, pp. 1–4.

[8] V. Giannini, P. Nuzzo, C. Soens, K. Vengattaramane, J. Ryckaert, M. Goffioul, B. Debaillie, J. Borremans, J. Van Driessche, J. Craninckx, and M. Ingels, "A 2-mm^2 0.1-5 GHz software-defined radio receiver in 45-nm digital CMOS," *IEEE Solid State J.*, vol. 44, no. 12, pp. 3486–3498, Dec. 2009.

[9] E. E. Djoumessi and K. Wu, "Electronically tunable diplexer for frequency-agile transceiver front-end," in *Proc. 2010 IEEE MTT-S Int. Microwave Symp.*, Anaheim, CA, May 23–28, 2010, pp. 1472–1475.

[10] C.-C. Cheng and G. M. Rebeiz, "A three-pole 1.2-2.6-GHz RF MEMS tunable notch filter with 40-dB rejection and bandwidth control," *IEEE Trans. Microwave Theory Tech.*, vol. 60, no. 8, pp. 2431–2438, Aug. 2012.

[11] Y.-C. Chiou and G. M. Rebeiz, "Tunable 1.55-2.1 GHz 4-pole elliptic bandpass filter with bandwidth control and rejection for wireless systems," *IEEE Trans. Microwave Theory Tech.*, vol. 61, no. 1, pp. 117–124, Jan. 2013.

[12] M. R. Naik and C. H. Vithalani, "Designing wideband voltage controlled oscillators for Software-Defined Radio," in *Proc. 2010 IEEE Int. Electronics, Circuits System Conf.*, Athens, Greece, pp. 1053–1056.

[13] J.-S. Hong, "Reconfigurable planar filters," *IEEE Microwave Mag.*, vol. 10, no. 6, pp. 73–83, Oct. 2009.

[14] A. C. Guyette, "Design of fixed- and varactor-tuned bandstop filters with spurious suppression," in *Proc. Microwave Conf., 2010 European*, Paris, France, pp. 288–291.

[15] J.-P. Magalhães, J. Vieira, R. Gómez-García, and N. B. Carvalho, "Bio-inspired hybrid filter bank for software-defined radio receivers," *IEEE Trans. Microwave Theory Tech.*, vol. 61, no. 4, pp. 1455–1466, Apr. 2013.

[16] J.-P. Magalhães, J. Vieira, R. Gómez-García, and N. B. Carvalho, "RF and IF channelizers for wide-band sensing in cognitive/software-defined-radio receivers," in *Proc. 42nd European Microwave Conf.*, Amsterdam, The Netherlands, Oct. 28–Nov. 2, 2012, pp. 1158–1161.

[17] R. Gómez-García, J.-M. Muñoz-Ferreras, and M. Sánchez-Renedo, "Multi-band pre-selectors for software-defined radio receivers," in *Proc. 2013 IEEE Radio Wireless Symp.*, Austin, TX, Jan. 20–23, 2013, pp. 13–15.

[18] J. A. Wepman, "Analog-to-digital converters and their applications in radio receivers," *IEEE Commun. Mag.*, vol. 33, no. 5, pp. 39–45, May 1995.

[19] S.-W. Sin, U. Seng-Pan, and R. P. Martins, "1.2-V, 10-bit, 60–360 MS/s time-interleaved pipelined analog-to-digital converter in 0.18 m CMOS with minimised supply headroom," *IET Circuits Devices Syst.*, vol. 4, no. 1, pp. 1–13, Jan. 2010.

[20] M. Mishali, Y. C. Eldar, O. Dounaevsky, and E. Shoshan, "Xampling: Analog to digital at sub-Nyquist rates," *IET Circuits Devices Syst.*, vol. 5, no. 1, pp. 8–20, Jan. 2011.

[21] J. Yian, S. W. Fung, K. Y. Chan, and R. Xu, "A 12-bit 20 MS/s 56.3 mW pipelined ADC with interpolation-based nonlinear calibration," *IEEE Trans. Circuits Syst. I, Reg. Papers*, vol. 59, no. 3, pp. 555–565, Mar. 2012.

[22] F. Cemturelli, P. Monsurro, and A. Trifiletti, "Efficient digital background calibration of time-interleaved pipeline analog-to-digital converters," *IEEE Trans. Circuits Syst. I, Reg. Papers*, vol. 59, no. 7, pp. 1373–1383, July 2012.

[23] D. F. Albuquerque, S. T. Soldado, J. M. N. Vieira, and N. B. Carvalho, "Cochlear radio," in *Proc. Wireless Technology Conf., 2010 European*, Paris, France, pp. 209–212.

[24] M. I. Skolnik, *Introduction to Radar Systems*, 3rd ed. New York: McGraw-Hill, 2002.

[25] L. Cai and H. Wang, "A persymmetric multiband GLR algorithm," *IEEE Trans. Aerosp. Electron. Syst.*, vol. 28, no. 3, pp. 806–816, July 1992.

[26] P. Lombardo and D. Pastina, "Multiband coherent radar detection against compound-Gaussian clutter," *IEEE Trans. Aerosp. Electron. Syst.*, vol. 35, no. 4, pp. 1266–1282, Oct. 1999.

[27] D. B. Trizna, C. Bachmann, M. Sletten, N. Allan, J. Toporkov, and R. Harris, "Projection pursuit classification of multiband polarimetric SAR land images," *IEEE Trans. Geosci. Remote Sensing*, vol. 39, no. 11, pp. 2380–2386, Nov. 2001.

[28] M. Vespe, C. J. Baker, and H. D. Griffiths, "Automatic target recognition using multi-diversity radar," *IET Radar, Sonar Navigat.*, vol. 1, no. 6, pp. 470–478, Dec. 2007.

[29] R. A. Romero and N. A. Goodman, "Waveform design in signal dependent interference and application to target recognition with multiple transmission," *IET Radar, Sonar Navigat.*, vol. 3, no. 4, pp. 328–340, Aug. 2009.

[30] X. L. Wei, Y. A. Zheng, Z. Z. Cui, and Q. L. Wang, "Multi-band SAR images fusion using the EM algorithm in contourlet domain," in *Proc. Int. Conf. Fuzzy Systems Knowledge Discovery*, vol. 1, pp. 502–506, Aug. 2007.

[31] V. Jain, F. Tzeng, L. Zhou, and P. Heydari, "A single-chip dual-band 22–29-GHz/77-81-GHz BiCMOS transceiver for automotive radars," *IEEE J. Solid-State Circuits*, vol. 44, no. 12, pp. 3469–3485, Dec. 2009.

[32] J.-W. Hang and C. Nguyen, "Development of a tunable multiband UWB radar sensor and its applications to subsurface sensing," *IEEE Sensors J.*, vol. 7, no. 1, pp. 51–58, Jan. 2007.

[33] Z. Li, W. Li, H. Lv, Y. Zhang, X. Jing, and J. Wang, "A novel method for respiration-like clutter cancellation in life detection by dual-frequency IR-UWB radar," *IEEE Trans. Microwave Theory Tech.*, vol. 2, no. 2, pp. 1–7, Feb. 2013.

[34] S. Velazquez, T. Nguyen, and S. Broadstone, "Design of hybrid filter banks for analog/digital conversion," *IEEE Trans. Signal Process.*, vol. 46, no. 4, pp. 956–967, Apr. 1998.

[35] D. Asemani, J. Oksman, and P. Duhamel, "Subband architecture for hybrid filter bank A/D converters," *IEEE J. Select. Topics Signal Process.*, vol. 2, no. 2, pp. 191–201, Apr. 2008.

[36] H. Hu, K.-L. Wu, and R. J. Cameron, "Stepped circular waveguide dual-mode filters for broadband contiguous multiplexers," *IEEE Trans. Microwave Theory Tech.*, vol. 61, no. 1, pp. 139–145, Jan. 2013.

[37] A. Panariello, M. Yu, and C. Ernst, "Ku-band high power dielectric resonator fillters," *IEEE Trans. Microwave Theory Tech.*, vol. 61, no. 1, pp. 382–392, Jan. 2013.

[38] C. Rauscher, "Efficient design methodology for microwave frequency multiplexers using infinite-array prototype circuits," *IEEE Trans. Microwave Theory Tech.*, vol. 42, no. 7, pp. 1337–1346, July 1994.

[39] M. Zewani and I. C. Hunter, "Design of ring-manifold microwave multiplexers," in *Proc. 2006 IEEE MTT-S Int. Microwave Symp.*, San Francisco, CA, June 11–16, 2006, pp. 909–912.

[40] C. J. Galbraith, R. D. White, L. Cheng, K. Grosh, and G. M. Rebeiz, "Cochlea-based RF channelizing filters," *IEEE Trans. Circuits Syst. I, Reg. Papers*, vol. 55, no. 4, pp. 969–979, Apr. 2008.

[41] C. J. Galbraith and G. M. Rebeiz, "Higher order cochlea-like channelizing filters," *IEEE Trans. Microwave Theory Tech.*, vol. 56, no. 7, pp. 1675–1683, July 2008.

[42] J. L. Brown, "Generalized sampling and the perfect reconstruction problem for maximally decimated filter banks," in *Proc. 1989 Int. Conf. Acoustics, Speech, Signal Processing*, pp. 1195–1198.

[43] P. -J. S. G. Ferreira, "Interpolation and the discrete Papoulis–Gerchberg algorithm," in *Proc. IEEE Acoustics Speech Signal. Conf.*, vol. 42, no. 10, pp. 2596–2606, Oct. 1994.

[44] D. Asemani and J. Oksman, "Influences of oversampling and analog imperfections on hybrid filter bank A/D converters," in *Proc. 49th IEEE Int. Circuits System Midwest Symp.*, Aug. 2006, pp. 123–126.

[45] S. Soldado, J. Vieira, D. Albuquerque, and T. Monteiro, "Controlling the reconstruction error in hybrid filter banks," in *Proc. IEEE 12th Int. Signal Advances Wireless Communication Workshop*, 2011, pp. 46–50.

[46] A. Gruget, M. Roger, V. T. Nguyen, C. Lelandais-Perrault, P. Benabes, and P. Loumeau, "Optimization of bandpass charge sampling filters in hybrid filter banks converters for cognitive radio applications," in *Proc. 20th European Circuits Theory Design Conf.*, Aug. 2011, pp. 785–788.

[47] J.-P. Magalhães, T. Monteiro, J. Vieira, R. Gómez-García, and N. B. Carvalho, "Papoulis-Gerchberg hybrid filter bank receiver for cognitive-/software-defined radio systems," in *Proc. 2013 IEEE Int. Circuits System Symp.*, Beijing, China, pp. 69–72.

[48] D. Lockie and D. Peck, "High-data-rate millimeter-wave radios," *IEEE Microwave Mag.*, vol. 10, no. 5, pp. 75–83, Aug. 2009.

[49] S. C. Chan, K. M. Tsui, K. S. Yeung, and T. I. Yuk, "Design and complexity optimization of a new digital IF for software radio receivers with prescribed output accuracy," *IEEE Trans. Circuits Syst. I, Reg. Papers*, vol. 54, no. 2, pp. 351–366, Feb. 2007.

[50] M. A. T. Sanduleanu, M. Vidojkovic, V. Vidojkovic, A. H. M. van Roermund, and A. Tasic, "Receiver front-end circuits for future generations of wireless communications," *IEEE Trans. Circuits Syst. II, Exp. Briefs*, vol. 55, no. 4, pp. 299–303, Apr. 2008.

[51] G. Hueber, R. Stuhlberger, and A. Springer, "An adaptive digital frontend for multimode wireless receivers," *IEEE Trans. Circuits Syst. II, Exp. Briefs*, vol. 55, no. 4, pp. 349–353, Apr. 2008.

[52] D. M. Akos, M. Stockmaster, J. B. Y. Tsui, and J. Caschera, "Direct bandpass sampling of multiple distinct RF signals," *IEEE Trans. Commun.*, vol. 47, no. 7, pp. 983–988, July 1999.

[53] C. A. DeVries and R. D. Mason, "Subsampling architecture for low power receivers," *IEEE Trans. Circuits Syst. II, Exp. Briefs*, vol. 55, no. 4, pp. 304–308, Apr. 2008.

[54] F. Rivet, Y. Deval, J.-B. Begueret, D. Dallet, P. Cathelin, and D. Belot, "A disruptive receiver architecture dedicated to software-defined radio," *IEEE Trans. Circuits Syst. II, Exp. Briefs*, vol. 55, no. 4, pp. 344–348, Apr. 2008.

[55] R. Barrak, A. Ghazel, and F. Ghannouchi, "Optimized multistandard RF subsampling receiver architecture," *IEEE Trans. Wireless Commun.*, vol. 8, no. 6, pp. 2901–2909, June 2009.

[56] M. Mishali and Y. C. Eldar, "From theory to practice: Sub-Nyquist sampling of sparse wideband analog signals," *IEEE J. Sel. Topics Signal Process.*, vol. 4, no. 2, pp. 375–391, Apr. 2010.

[57] J.-M. Muñoz-Ferreras, R. Gómez-García, and F. Pérez-Martínez, "RF front-end concept and implementation for direct sampling of multi-band signals," *IEEE Trans. Circuits Syst. II, Exp. Briefs*, vol. 58, no. 3, pp. 129–133, Mar. 2011.

[58] J.-M. Muñoz-Ferreras, R. Gómez-García, and F. Pérez-Martínez, "Multi-band radar receiver design approach for minimum bandpass sampling," *IEEE Trans. Aerospace Electronic Syst.*, vol. 49, no. 2, pp. 774–785, Apr. 2013.

[59] L. Y. Ren, "Quad-band bandpass filter based on dual-plane microstrip/DGS slot structure," *Electron. Lett.*, vol. 46, no. 10, pp. 691–692, May 2010.

[60] J. C. Liu, J.-W. Wang, B.-H. Zeng, and D.-C. Chang, "CPW-fed dual-mode double-square-ring resonators for quad-band filters," *IEEE Microwave Wireless Compon. Lett.*, vol. 20, no. 3, pp. 142–144, Mar. 2010.

[61] J. Xu, W. Wu, and C. Miao, "Compact microstrip dual-/tri-/quad-band bandpass filter using open stubs loaded shorted stepped-impedance resonator," *IEEE Trans. Microwave Theory Tech.*, vol. 61, no. 9, pp. 3187–3199, Sept. 2013.

[62] R. Gómez-García, J.-M. Muñoz-Ferreras, and M. Sánchez-Renedo, "Microwave transversal six-band bandpass planar filter for multi-standard wireless applications," in *Proc. 2011 IEEE Radio Wireless Symp.*, Phoenix, AZ, pp. 166–169.

[63] R. Gómez-García, J.-M. Muñoz-Ferreras, and M. Sánchez-Renedo, "Signal-interference stepped-impedance-line microstrip filters and application to duplexers," *IEEE Microwave Wireless Compon. Lett.*, vol. 21, no. 8, pp. 421–423, Aug. 2011.

[64] M. A. Richards, J. A. Scheer, and W. A. Holm, *Principles of Modern Radar. Basic Principles*, 2nd ed. Edison, NJ: SciTech Publishing, 2010.

[65] A. Blanco-del-Campo, A. Asensio-López, J. Gismero-Menoyo, B. P. Dorta-Naranjo, and J. Carretero-Moya, "Instrumental CWLFM high-range resolution radar in millimeter waveband for ISAR imaging," *IEEE Sens. J.*, vol. 11, no. 2, pp. 418–429, Feb. 2011.

[66] W. G. Carrara, R. S. Goodman, and R. M. Majewski, *Spotlight Synthetic Aperture Radar: Signal Processing Algorithms*. Norwood, MA: Artech House, 1995.

[67] E. C. Zaugg, D. L. Hudson, and D. G. Long, "The BYU μSAR: A small, student-built SAR for UAV operation," in *Proc. Int. Geoscience Remote Sensing Symp.*, Denver, CO, Aug. 2006, pp. 411–414.

[68] P. Almorox-Gonzalez, J. T. González-Partida, M. Burgos-García, C. de la Morena-Álvarez-Palencia, L. Arche-Andradas, and B. P. Dorta-Naranjo, "Portable high resolution LFM-CW radar sensor in millimeter-wave band," in *Proc. 2007 Int. Conf. Sensor Technologies Applications*, Valencia, Spain, pp. 5–9.

[69] M. Edrich, "Design overview and flight test results of the miniaturised SAR sensor MISAR," in *Proc. 1st European Radar Conf.*, Amsterdam, The Netherlands, Oct. 2004, pp. 205–208.

[70] D. R. Wehner, *High-Resolution Radar*, 2nd ed. Norwood, MA: Artech House, 1995.

[71] C. C. Chen and H. C. Andrews, "Target motion induced radar imaging," *IEEE Trans. Aerosp. Electron. Syst.*, vol. 16, no. 1, pp. 2–14, Jan. 1980.

[72] D. A. Ausherman, A. Kozma, J. L. Walker, H. M. Jones, and E. C. Poggio, "Developments in radar imaging," *IEEE Trans. Aerosp. Electron. Syst.*, vol. 20, no. 4, pp. 363–399, Aug. 1984.

[73] J. M. Muñoz-Ferreras and F. Pérez-Martínez, "Uniform rotational motion compensation for inverse synthetic aperture radar with non-cooperative targets," *IET Radar, Sonar Navigat.*, vol. 2, no. 1, pp. 25–34, Jan. 2008.

[74] J. M. Muñoz-Ferreras, F. Pérez-Martínez, and M. Datcu, "Generalisation of inverse synthetic aperture radar autofocusing methods based on the minimisation of the Rényi entropy," *IET Radar, Sonar Navigat.*, vol. 4, no. 4, pp. 586–594, Aug. 2010.

[75] J. M. Muñoz-Ferreras and R. Gómez-García, "Approaches for linear-frequency-modulated continuous-wave (LFMCW) dual-band radars," in *Proc. European Radar Conf.*, Nuremberg, Germany, Oct. 2013, pp. 204–207.

[76] J. M. Muñoz-Ferreras and R. Gómez-García, "A deramping-based multi-band radar sensor concept with enhanced ISAR capabilities," *IEEE Sensors J.*, vol. 13, no. 9, pp. 3361–3368, Sept. 2013.